Comparison of the reluctance laminated and solid rotor synchronous machine operating at high temperatures

Marcin Lefik, Krzysztof Komeza, Ewa Napieralska-Juszczak, Daniel Roger, Piotr Napieralski

Comparison of the reluctance laminated and solid rotor synchronous machine operating at high temperatures.

Marcin Lefik, Krzysztof Komeza, Ewa Napieralska-Juszczak, Daniel Roger,Poitr Andrej Napieralskik

Abstract
Purpose – The purpose of this paper is to present a comparison between reluctance synchronous machine-enabling work at high internal temperature (HT° machine) with laminated and solid rotor.
Design/methodology/approach – To obtain heat sources for the thermal model, calculations of the electromagnetic field were made using the Opera 3D program including effect of rotation and the resulting eddy current losses. To analyze the thermal phenomenon, the 3D coupled thermal-fluid (CFD) model is used.
Findings – The presented results show clearly that laminated construction is much better from a point of view of efficiency and temperature. However, solid construction can be interesting for high speed machines due to their mechanical robustness.
Research limitations/implications – The main problem, despite the use of parallel calculations, is the long calculation time.
Practical implications – The obtained simulation and experimental results show the possibility of building a machine operating at a much higher ambient temperature than it was previously produced for example in the vicinity of the aircraft turbines.
Originality/value – The paper presents the application of fully three-dimensional coupled electromagnetic and thermal analysis of new machine constructions designed for elevated temperature.

Keywords : Electrical machine, Thermal analysis, Finite element method.

Paper type : Research paper

1. Introduction

High-temperature (HT) electrical machines are intended for specific applications. They are designed to work at higher temperatures than those typically used. Of course, in such an environment, the temperature within the machine also increases. For example, the synchronous reluctance motor (SynRM) designed for aircraft applications works at ambient temperature of around 200°C, whereas the temperature within the motor's frame reaches 450-500°C at the hottest spot. With electrical machines capable of running in such an environment, engine manufacturers have been able to reduce the reliance on mechanically driven accessories and, according to the More Electrical Engine concept, provide a better product in terms of efficiency and reliability. Continuous operation in such conditions requires the use of inorganic Electrical Insulation Systems (EIS), as traditional organic materials are not capable of withstanding such a high temperature, and an architecture adjusted to the inorganic insulation technology (Iosif et al., 2016a, 2016b; Cozonac et al., 2014). This topology allows two main options: permanent magnet synchronous machine or synchronous reluctance machine, in which the torque is generated through the phenomenon of magnetic reluctance (Pyrhoonen et al., 2008; Belhadi et al., 2015; Lipo, 1991). The HT engine built of rigid inorganic coils requires a special stator construction with rectangular teeth shape and open slots. Therefore, design calculations of these electromechanical transducers must be preceded by a specific thermal and electromagnetic analysis, aimed to estimate the thermal effects of power loss. This paper presents a 3D FEM-based electromagnetic and thermal analysis of the HT synchronous reluctance machine (SynRM) working with the rotational speed 4800 rpm. The analysis relies on 3D computational fluid dynamics (CFD). Due to the specific stator design linked to the coil winding technology and a large number of poles, the choice of the rotor construction was fairly limited. The present study is based on a salient pole type of rotor. To increase the torque, the poles were notched lengthwise and a round opening at the base of the rotor tooth was added to serve as a flux barrier. Figure 1 shows the main parts of the reluctance motor. Both electromagnetic and CFD solutions take into account changes in parameters and characteristics of materials associated with high operating temperature (Cozonac et al., 2014; Finger and Rubertus, 2000; Ababsa et al., 2018; Komeza et al., 2016, 2017).

The rotor can be made as a solid or as a laminated. Solid construction is mechanically more robust allowing higher rotation speed; moreover, induced currents can generate torque during starting. Unfortunately, stator construction, even with used stator slot wedges, generates higher flux harmonics which produced high losses in rotor at synchronous speed. Induced in solid rotor poles currents weakened the effect of reluctance changes. Figure 2 shows comparison of torque versus load angle for both: laminated and solid design. Evidently, a motor with a massive rotor has a much smaller synchronous torque as well as a smaller range of stable operation. This is due to the effect of shielding the rotor through currents induced in its structure.

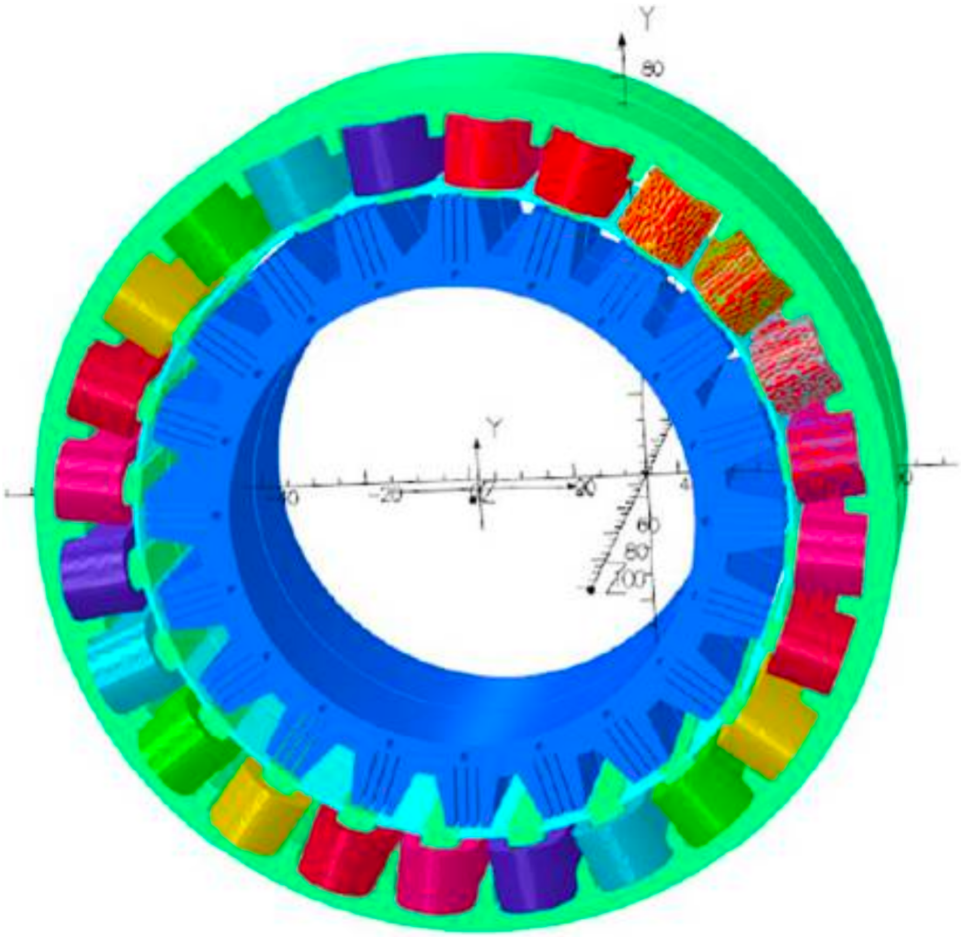

Figure 1. Reluctance motor.

2. Electromagnetic field simulation

To obtain heat sources for the thermal model, calculations of the electromagnetic field were made using the Opera 3D program. As commonly known the 3D time-stepping FEM is very time-consuming (Ionel and Popescu, 2010; Bianchi et al., 2013; Ponomarev et al., 2014); thus, the use of 2D analysis is preferred (El-Refaie, 2010; Komeza et al., 2016; El-Refaie and Jahns, 2005; Tang et al., 2015). The time-stepping analysis was performed over approximately 20 cycles until the steady state was reached. First, 2D and after 3D simulation were realized. For the purpose of the 3D simulation, a quarter of the machine has been considered to benefit from the magnetic symmetry. The time- stepping analysis was performed assuming constant speed of rotation of the rotor. Magnetic vector potential formulation with linear edge elements was used in that analysis. The analysis relies upon a remeshing technique. During the transient analysis, before the solution at the next time-step, the position of each moving part is updated. The 3D mesh contains 4.264778 million elements in total (including 700,000 in gap region). In the conductive areas, the elements size was chosen to be less than one- third of the penetration depth. Moreover, the distribution of the density of the mesh is greater than to correctly reproduce the effect of rotation of the rotor relative to the stator. To reduce the computation times, the simulations were performed on a virtual machine with eight cores. Figure 3 shows finite element mesh for 3D model of the quarter of the machine.
Figure 4(a) and 4(b) shows the comparison of torque for laminated and solid rotor (made from steel C10) calculated by 2D and 3D models. While for laminated rotor, 2D and 3D results were almost the same, for solid rotor, they differ significantly.
The reason for such a large difference between a 3D and 2D solution for a motor with a massive rotor is the complex distribution of currents [show in Figure 5(a)], and the resulting changes in the magnetic flux density distribution [Figure 5(b)]. Only in the stator area as shown in Figure 6(a), the field distribution is analogous as for the motor with laminated rotor [Figure 6(b)].
Even for synchronous speed, higher harmonics cause significant losses in the conductive material of the rotor (despite the elevated temperature the conductivity is 2.24 MS/m). Figure 7 shows rotor losses versus time for one period. The total losses in the rotor are practically independent of the load angle and amount to 1030 W for the maximum torque.

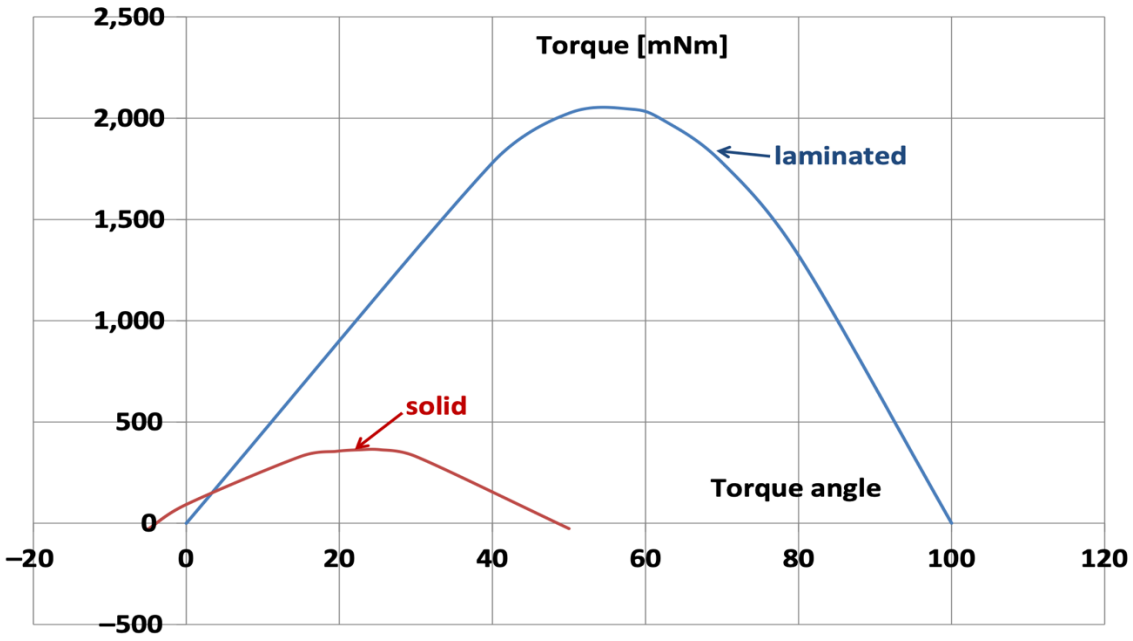

Figure 2. The comparison of torque for laminated and solid rotor design.

3. 3D coupled thermal fluid model

To analyse the thermal phenomenon, the 3D coupled thermal-fluid (CFD) model is used (Unai et al., 2014; Arbab et al., 2015). The CFD model allows to calculate the distribution of the temperature field and average temperature of the windings and the other motor's parts. In addition, this model can be used to localize points with the highest value of the temperature (hot points). The CFD model is based on the Reynolds-averaged Navier– Stockes equations (RANS equations) for the steady flow. RANS equations can be written as follows (Grybos, 1998):

$$\nabla \bar{v} = 0 \tag{1}$$

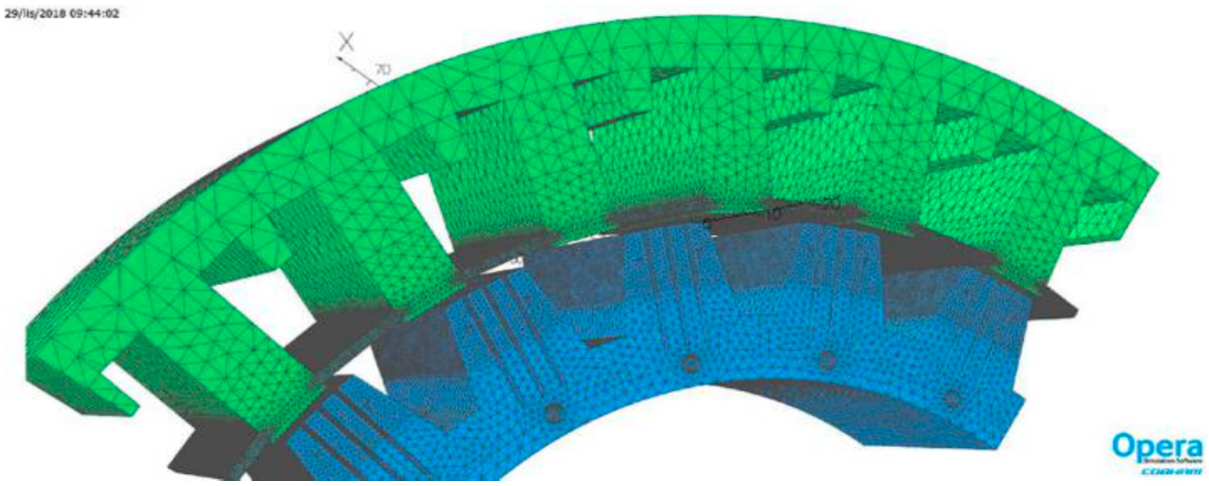

Figure 3. Finite element mesh for 3D model of the quarter of the machine contains 4.264778 million elements.

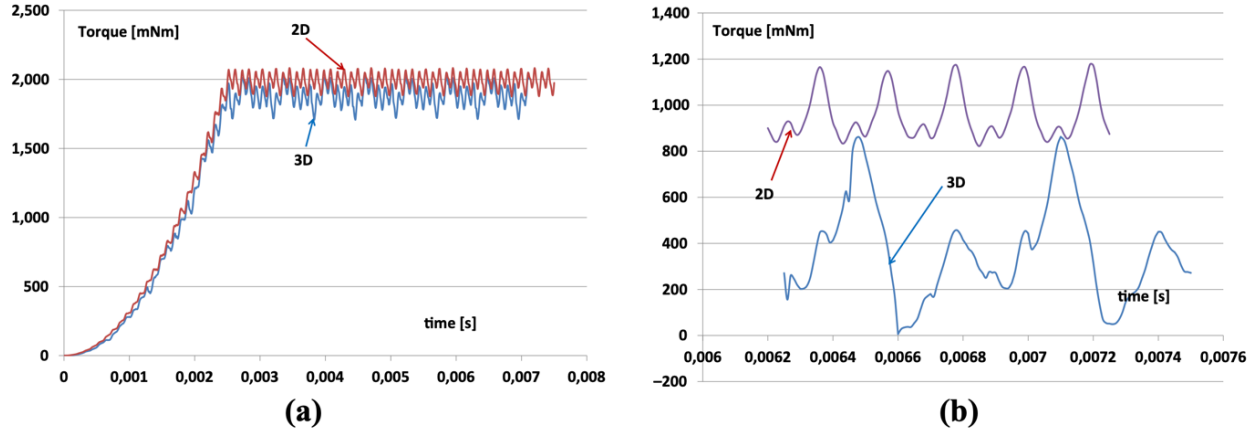

Figure 4. Comparison of torque 1,500 for laminated rotor design calculated by 1,000 2D and 3D models (a), Comparison of torque or solid rotor design calculated by 2D and 3D models (b).

$$\mu \nabla^2 \overline{v} = \nabla \overline{p} + \nabla \overline{\tau} \tag{2}$$

$$\frac{\kappa}{c\,\rho} \nabla^2 \overline{T} + \frac{\kappa}{c\,\rho} \left(\overline{D} + Q\right) - \nabla \overline{\nu T} - \nabla \overline{\nu' T'} = 0 \tag{3}$$

where V is an averaged values of fluid velocity, P is averaged values of fluid pressure, T is averaged values of fluid temperature, Q is a heat source density, t is a Reynolds-stress tensor, D is an intensity of dissipation and k; c; r; m are thermal conductivity, specific heat, mass density and dynamic viscosity, respectively.

Equations (1)-(3) can be solved only with turbulence models. The most commonly used types of turbulence models are k-« models. The k-« models include two additional differential equations which are written for turbulent kinetic energy k and dissipation «. In analysed case k-« Realizable turbulent model is used. In rotation machines, it is necessary to take into account the rotor rotation and thermal radiation. Both phenomena affect the heat flow in analysed machines. Rotation of the machines rotor can be modelled using multiple rotating reference frames (MRF model), where the equations for rotor are written in moving reference frame and for the other machine's parts in stationary reference frame. Radiation inside the machine's housing can be included by radiation model, for example discrete ordinates, and for external walls by combined boundary condition for energy equation with the surface emissivity coefficient «$_r$. Combined boundary condition is given by following formula [18]:

$$-\kappa \frac{\partial T}{\partial n} = h_c \left(T_w - T_\infty\right) + \varepsilon_r \sigma \left({T_w}^4 - {T_{ext}}^4\right) \tag{4}$$

where h_c is a convective heat transfer coefficient, T_1 is temperature of the ambient air, T_w is surface temperature of the wall, T_{ext} is the ambient temperature and s is the Stefan– Boltzmann constant. The convective heat transfer coefficient h_c can be determined from empirical formula which is based on dimensionless Rayleigh and Nusselt numbers.

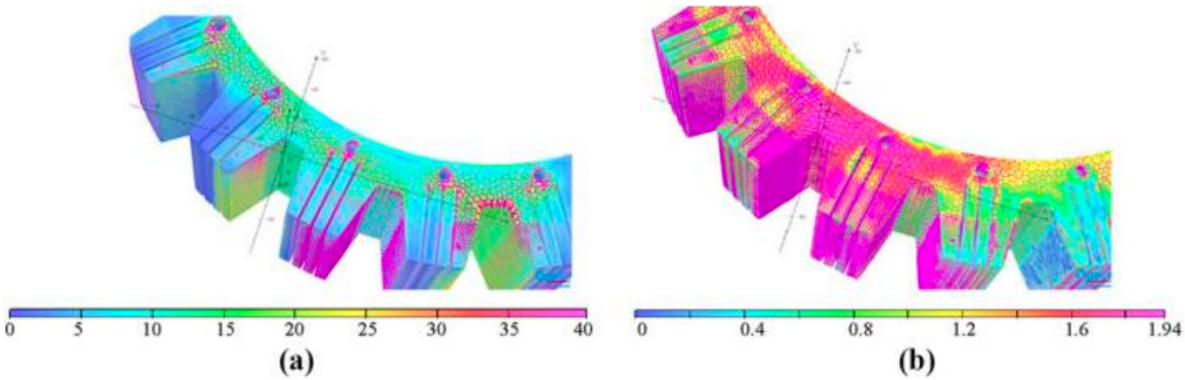

Figure 5. The distribution of current induced in solid rotor [A/mm^2] (a); the distribution of magnetic flux density [T] (b).

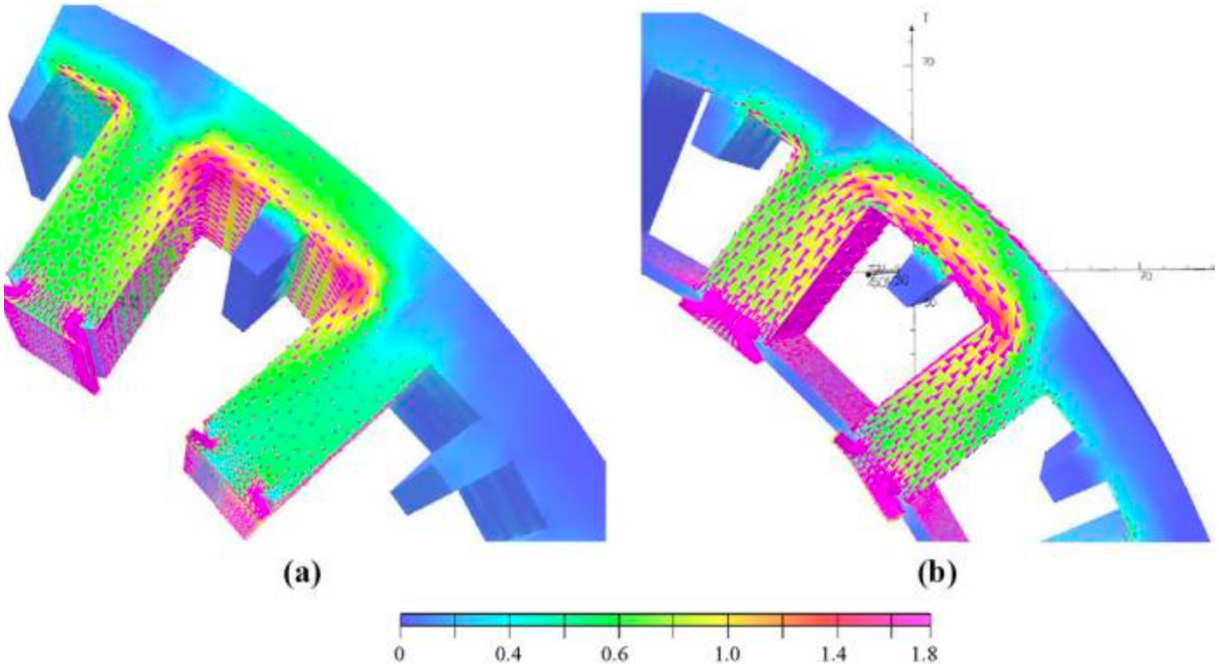

Figure 6. The distribution of magnetic flux density in stator: for the motor with solid rotor (a); for the motor with laminated rotor (b)

Figure 7. Solid rotor losses versus time for one period.

3D coupled thermal-fluid model is prepared using Ansys Fluent package. Solid model of HT° reluctance synchronous machine is shown on Figure 8(a) and 8(b). This model includes such parts as housing, shaft, bearings. These machine's elements should not be omitted because they participate in the heat flow in the machine. The 3D finite volume mesh of the analyzed HT° machine model has 4475389 tetrahedral elements. The 3D mesh is presented on Figure 8(c).

Heat sources in the analyzed machine are the power losses. The power losses in the core and windings of HT° reluctance synchronous machine were calculated. In equation (3), the heat source is presented as heat source density Q. It can be calculated from following formula:

$$Q = \frac{\Delta P}{V} \tag{5}$$

where DP is power losses taken from electromagnetic calculations, whereas V is a volume of motor's part where these power losses were generated.

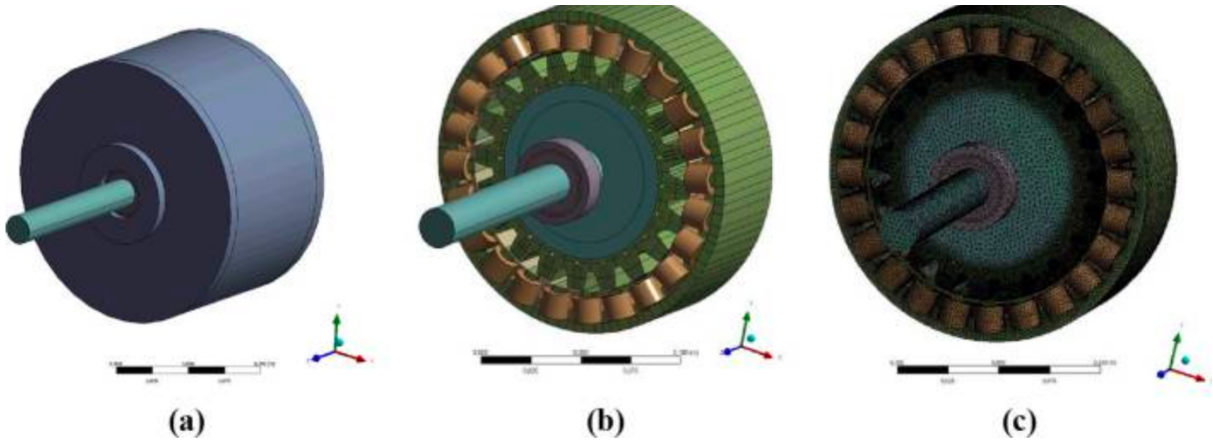

Figure 8. Solid model of HT° reluctance synchronous machine (a), (b), 3D finite volume mesh (c).

4. Results of the thermal analysis

Thermal analysis allowed to compare thermal phenomena occurring in both variants of the designed machine. Thermal field distributions in machines and average temperature values of individual machines parts for two values of ambient temperature (200°C and 500°C) were calculated. In these calculations, the effect of temperature on the change of winding resistance, solid rotor conductivity and the associated change in power losses was taken into account. The results of thermal analysis in Table I, Figures 9 and 10 were shown.

The obtained results show that machine with solid rotor has higher values of temperature than machine with laminated rotor. Additional losses in solid rotor cause that other elements of this machine they overheat, in particular the winding coils. The average value of the winding temperature for a laminated rotor at an ambient temperature of 200°C is 393.8°C, while for a solid rotor it is 558.6°C. As can be seen in the case of the massive rotor, the estimated operating temperature (450-500°C) of the coils is exceeded. A similar situation exists for the machine operating at ambient temperature 500°C. The average temperature is 612.9°C for machine with laminated rotor and 697.2°C for solid rotor.

Table I. Temperature values for selected machine components for laminated and solid rotors

		Ambient temperature 200°C				Ambient temperature 500°C			
		Laminated		Solid		Laminated		Solid	
No.	Machine's part name	°C	K	°C	K	°C	K	°C	K
1	Rotor package	354.6	627.6	618.1	891.1	579.1	852.1	736.8	1009.8
2	Stator package	350.7	623.7	504.0	777.0	576.9	849.9	651.6	924.6
3	Winding	393.8	666.8	558.6	831.6	612.9	885.9	697.2	970.2
4	Housing	339.4	612.4	475.9	748.9	564.0	837.0	624.9	897.9

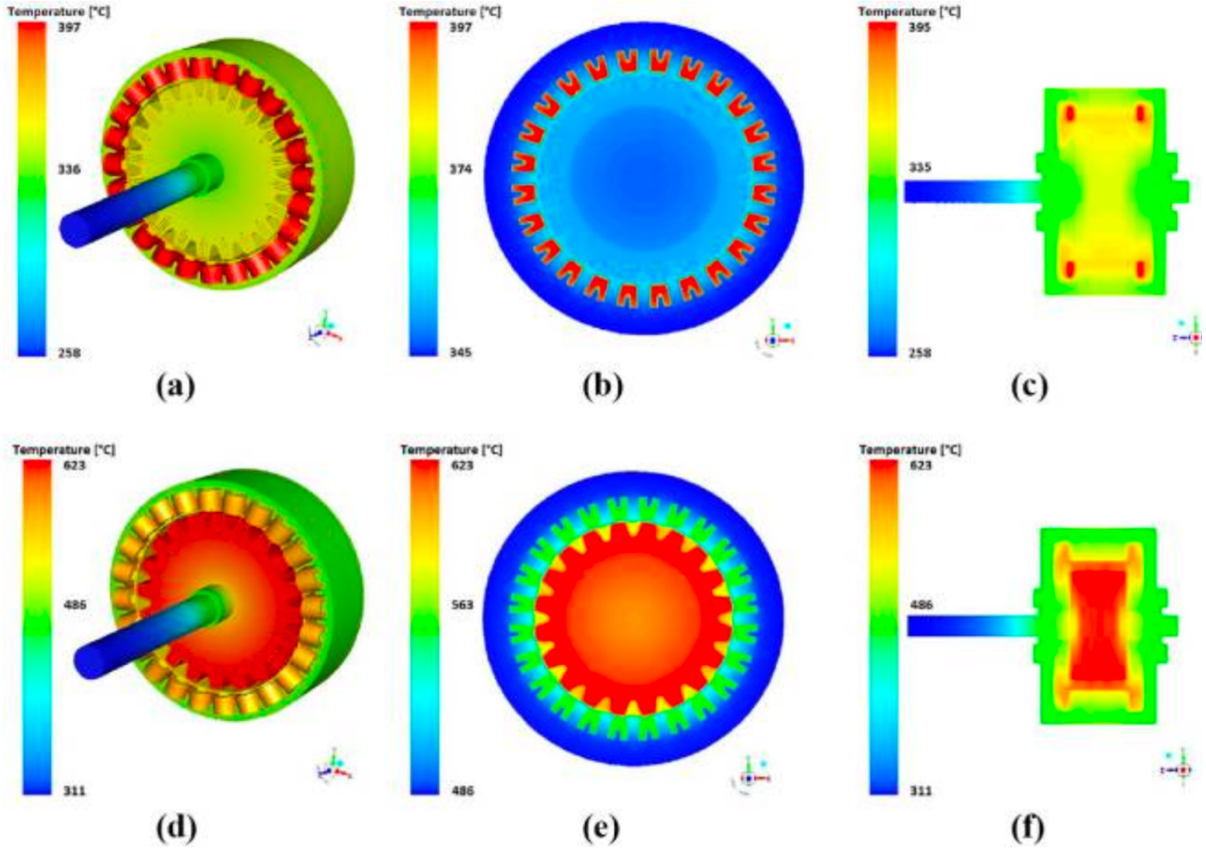

Figure 9. Temperature distribution in machine with laminated (a), (b), (c) and solid (d), (e), (f) rotor for the ambient temperature 200°C.

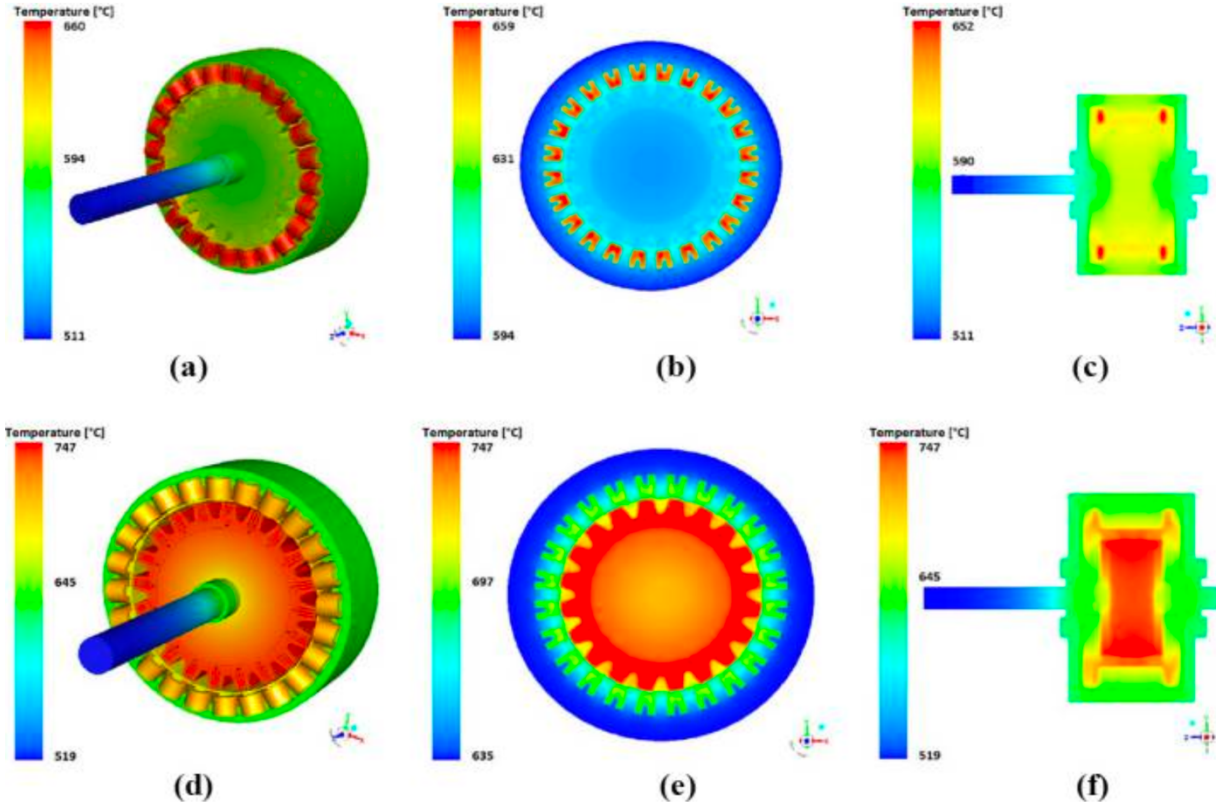

Figure 10. Temperature distribution in machine with laminated (a), (b), (c) and solid (d), (e), (f) rotor for the ambient temperature 500°C.

5. Summary

In this study, we analyzed the influence of the design of the rotor (solid or laminated) on efficiency and temperature of the motor active parts. The presented results show clearly that laminated construction is much better from a point of view of efficiency and temperature. However, solid construction can be interesting for high-speed machines due to their mechanical robustness.
The influence of ambient temperature on the winding's coils temperature was also analysed. The results have shown that the optimal temperature for the machine with laminated rotor is 200°C. In this case, the average temperature of the coils is 393.8°C, while the estimated operating temperature of the coils is 450-500°C. The coils are overheated for a higher ambient temperature.

References

Ababsa, M.L., Ninet, O., Velu, G. and Lecointe, J.P. (2018), "High-temperature magnetic characterization using an adapted epstein frame", IEEE Transactions on Magnetics, Vol. 54 No. 6.
Arbab, N., Wang, W., Lin, C., Hearron, J. and Fahimi, B. (2015), "Thermal modeling and analysis of a double-stator switched reluctance motor", IEEE Transactions on Energy Conversion, Vol. 30 No. 3, pp. 1209-1217.
Belhadi, M.H., Krebs, G., Marchand, C., Hannoun, H. and Mininger, X. (2015), "Switched reluctance motor with magnetic slot wedges for automotive traction application", European Physical Journal of Applied Physics EPJAP, pp. 1-6.
Bianchi, N., Durello, D. and Fasolo, A. (2013), "Relationship between rotor losses and size of permanent- magnet machines", IEEE Transactions on Industry Applications, Vol. 49 No. 5, pp. 2015-2023. Cozonac, D., Lecointe, J.P., Duchesne, S. and Velu, G. (2014), "Materials characterization and geometry
of a high temperature induction machine", 2014 International Conference on Electrical Machines
(ICEM), pp. 2499-2505.
El-Refaie, A.M. (2010), "Fractional-slot concentrated-windings synchronous permanent magnet machines:
opportunities and challenges", IEEE Transactions on Industrial Electronics, Vol. 57 No. 1, pp. 107-121. El-Refaie, A.M. and Jahns, T.M. (2005), "Optimal flux weakening in surface PM machines using fractional-
slot concentrated windings", IEEE Transactions on Industry Applications, Vol. 41 No. 3.
Finger, R.T. and Rubertus, C.S. (2000), "Application of high temperature magnetic materials", IEEE
Transactions on Magnetics, Vol. 36, pp. 3373-3375.
Grybos, R. (1998), Fundamentals of Fluid Dynamics: Part 1 (in Polish), PWN, Warszawa.
Ionel, D.M. and Popescu, M. (2010), "Finite element surrogate model for electric machines with
revolving field – application to IPM motors", IEEE Transactions on Industry Applications,
Vol. 46 No. 6, pp. 2424-2433.
Iosif, V., Roger, D., Duchesne, S. and Malec, D. (2016a), "An insulation solution for coils of high temperature
motors (500°C)", 2016 IEEE International Conference on Dielectrics (ICD), Vol. 1, pp. 297-300.
Iosif, V., Roger, D., Duchesne, S. and Malec, D. (2016b), "Assessment and improvements of inorganic insulation for high temperature low voltage motors", IEEE Transactions on Dielectrics and Electrical Insulation, Vol. 23 No. 5, pp. 2534-2542.
Komeza, K., Napieralska Juszczak, E., Roger, D., Takorabet, N., Meibody-Tabar, F. and Lefik, M. (2016), "Analysis of the impact of the design of HT machines on the cogging torque and losses in permanent magnets", IEEE International Conference on Power Electronics, Drives and Energy Systems IEEE PEDES 2016.
Komeza, K. Napieralska Juszczak, E. Roger, D. Takorabet, N. Meibody-Tabar, F. and Lefik, M. (2017), "Numerical analysis of thermal and mechanical field in the high temperature permanent magnet synchronous machine", ITEC2017.
Lipo, T.A. (1991), "Synchronous reluctance machines: a viable alternative for A.C. drives?", Electronics Machines Power Systems, Vol. 19 No. 6, pp. 659-671.
Ponomarev, P., Petrov, I. and Pyrhonen, J. (2014), "Influence of travelling current linkage harmonics on inductance variation torque ripple and sensorless capability of tooth-coil permanent-magnet synchronous machines", IEEE Transactions on Magnetics, Vol. 50 No. 1, pp. 1-8.
Pyrhoonen, J., Jokinen, T. and Hrabovcova, V. (2008), Design of Rotating Machines, John Wiley and Son.
Tang, C., Soong, W.L., Jahns, T.M. and Ertugrul, N. (2015), "Analysis of iron loss in interior pm machines with distributed windings under deep field weakening", IEEE Transactions on Industry Applications, Vol. 51 No. 5, pp. 3761-3772.
Unai, S., Gaizka, A., Javier, P. and Gaizka, U. (2014), "Design of cooling systems using computational fluid dynamics and analytical thermal models", IEEE Transactions on Industrial Electronics, Vol. 61 No. 8, pp. 4383-4391.

Further reading: Ansys Fluent 17.2 (2016), Theory Guide, Ansys Fluent 17.2.

Corresponding author: Komeza Krzysztof can be contacted at: krzysztof.komeza@p.lodz.pl